

---

# Zero-shot Inversion Process for Image Attribute Editing with Diffusion Models

---

Zhanbo Feng<sup>\*1</sup>Zenan Ling<sup>\*†2</sup>Ci Gong<sup>2</sup>Feng Zhou<sup>3</sup>Jie Li<sup>1</sup>Robert C. Qiu<sup>2</sup><sup>1</sup> Department of Computer Science and Engineering, Shanghai Jiao Tong University<sup>2</sup> EIC, Huazhong University of Science and Technology<sup>3</sup> Center for Applied Statistics and School of Statistics, Renmin University of China

## Abstract

Denoising diffusion models have shown outstanding performance in image editing. Existing works tend to use either image-guided methods, which provide a visual reference but lack control over semantic coherence, or text-guided methods, which ensure faithfulness to text guidance but lack visual quality. To address the problem, we propose the Zero-shot Inversion Process (ZIP), a framework that injects a fusion of generated visual reference and text guidance into the semantic latent space of a *frozen* pre-trained diffusion model. Only using a tiny neural network, the proposed ZIP produces diverse content and attributes under the intuitive control of the text prompt. Moreover, ZIP shows remarkable robustness for both in-domain and out-of-domain attribute manipulation on real images. We perform detailed experiments on various benchmark datasets. Compared to state-of-the-art methods, ZIP produces images of equivalent quality while providing a realistic editing effect.

## 1 Introduction

Manipulating real-world images with natural language has long been a challenge in image processing. Recently, denoising diffusion models (DDMs) have shown substantial success in text-to-image tasks, such as Imagen (Saharia et al., 2022), Dall-E (Ramesh et al., 2021), and Stable Diffusion (Rombach et al., 2022). These text-to-image models produce diverse, highly coherent, and realistic images that align well with text prompts. However, attribute manipulation on real images is still a challenging problem. In this paper, we aim to utilize these novel foundational models to manipulate real images in a controllable and semantically coherent manner.

Figure 1(a) and Figure 1(b) briefly illustrate currently popular methodologies. On the one hand, much effort has been put into text-guided image editing. Along with the development of the Natural Language Processing (NLP) technique, e.g., Generative Pre-Training (GPT) (OpenAI, 2023; Brown et al., 2020), many previous works (Bao et al., 2023; Hertz et al., 2022) develop image-editing techniques with the guidance of textual prompts. However, the importance of the visual reference is ignored in these methods. Though text-guided methods maintain faithfulness to the target semantic, it is difficult to learn fine-grained visual patterns from textual features in the absence of a visual prior. Using textual semantics alone lacks visual reference, resulting in sketchy semantic manipulation. Especially if the desired semantic is out of the domain, text-guided editing fails.

---

<sup>\*</sup> Equal contribution.

<sup>†</sup> Corresponding author. Email: lingzenan@hust.edu.cn

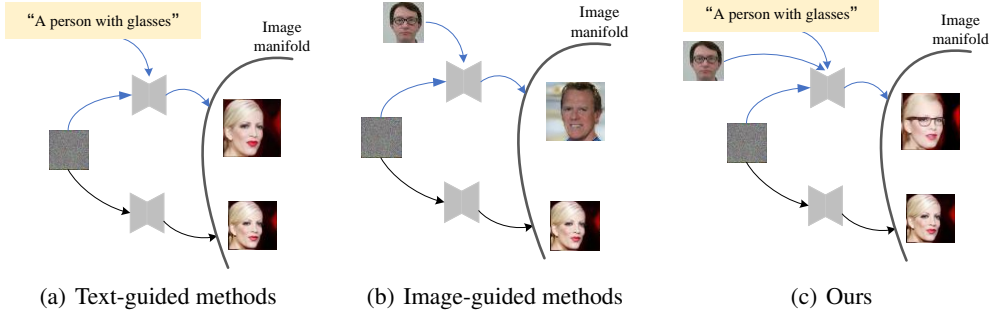


Figure 1: **Editing methods for denoising diffusion models.** (a) Text-guided methods cannot generate out-of-domain visual features. (b) Image-guided methods suffer ambiguity and distorted results. (c) Our method achieves specific and high-quality manipulation.

On the other hand, image-guided methods attract a large amount of attention. Image-guided editing can easily make style transfer (Choi et al., 2021) and item replacement (Jia et al., 2023). With visual reference, generators can directly insert ready-made visual patterns into images. However, as illustrated in Figure 1(b), image-guided approaches lack intuitive control over semantic coherence, and it is ambiguous to specify which attribute to refer from the reference image.

In this paper, we propose Zero-shot Inversion Process (ZIP) that injects a fusion of generated visual reference and text guidance into the semantic latent space of a *frozen* pre-trained diffusion model. As illustrated in Figure 1(c), our method takes advantage of the text guidance to provide intuitive control over the semantic coherence. Meanwhile, our methods refine the alignment of the text feature and the semantic latent space of the diffusion model by incorporating a visual reference. The incorporated reference image is generated with a foundational text-to-image model. Thus, our method is zero-shot and avoids the bias of manual selection. To the best of our knowledge, it is the first attempt to integrate text guidance and image guidance in zero-shot image editing. Our method only needs to train an attribute encoder, a tiny neural network, without fine-tuning the pre-trained model. For both in-domain and out-of-domain attribute editing tasks, our method preserves faithfulness to text guidance while maintaining visual quality. Extensive experiments demonstrate that our method is generally applicable to various benchmark datasets (CelebA-HQ, LSUN-church, and LSUN-bedroom).

## 2 Related Work

**Text-to-Image Synthesis:** Since the success of large language models, text prompts are widely used in image editing. Benefiting from the semantic information of text, Stable Diffusion (Rombach et al., 2022) makes a powerful and flexible generator with the condition of the text. Diffusionclip (Kim et al., 2022) shows that a textual prompt allows DDMs to edit the images in a semantic latent space. Asymp (Kwon et al., 2022) reveals that diffusion models already have a semantic latent space. Imagen Editor (Wang et al., 2022) uses the masks as input to point out the area of edit in the image, which can gather up the semantic information into the target. Though these works show a significant process in the editing of some attributes, only by text prompt, they just can generate ordinary attributes such as colors or common shapes in the image. To generate new visual features, such as glasses and other decorations in the images, the visual information should be taken into account.

**Image-to-Image Synthesis:** In contrast, image-guided approaches use the reference image as a condition to generate corresponding images. On the one hand, the features from the reference image are used to adjust the target image. There are many typical tasks such as style transfer (Choi et al., 2021; Meng et al., 2021) and inpainting (Lugmayr et al., 2022), where the reference image is viewed as an auxiliary feature. SDEdit (Meng et al., 2021) uses the stroke-based images to generate faithful images with the original images. On the other hand, the reference image is directly inserted into the target image. Jia et al. (2023) makes remarkable performance by using the reference image for personalized syntheses, such as the replacement of the items. Mystyle (Nitzan et al., 2022) adopts a pre-trained StyleGAN for personalized face generation by using the images of the generic face prior.

However, due to the ambiguity of the attribute choice in one image, image-guided approaches often make distorted images or incorrect manipulation. By using the text prompt, our ZIP circumvents this drawback with the alignment of visual features and semantic information from text.

**Attribute Editing** Many previous works (Kwon et al., 2022; Wallace et al., 2022; Daras and Dimakis, 2022) have focused on image editing based on large-scale generative models. On the one hand, these models mainly focus on editing DDM-generated images rather than real images. By adding, replacing, or modifying corresponding features, Prompt2prompt (Hertz et al., 2022) can change the items of a DDM-generated image. However, it is difficult to learn textual features corresponding to the real image. On the other hand, some models can only achieve sketchy editing for real images. For example, the background replacement is made in Direct Inversion (Elarabawy et al., 2022). The replacement of items in the real images is achieved in Jia et al. (2023). Some in-domain attributes, such as the age, gender, and expression of humans, are modified by Asymp (Kwon et al., 2022). However, these models are incomplete for the attributes which need both visual and semantic information such as wearing glasses.

### 3 Preliminary

#### 3.1 Diffusion Model

Denoising diffusion models (DDMs) produce more realistic samples than deep generative models before, such as GANs (Karras et al., 2020). A typical DDM includes two stages: the forward process to add Gauss noise to the original data and the reverse process to denoise samples until an image. Denoising Diffusion Probabilistic Model (DDPM) (Ho et al., 2020), starting from white noise, progressively denoises it into an image. Denoising Diffusion Implicit Models (DDIM) (Song et al., 2020a) reduce the number of iterations by taking generated results of different stages into the condition of generation.

The forward process diffuses the original data  $x_0$  with Gaussian noise, indexed by a real vector  $\sigma \in \mathbb{R}_{\geq 0}^T$ :

$$q_\sigma(x_{1:T}|x_0) := q_\sigma(x_T|x_0) \prod_{t=2}^T q_\sigma(x_{t-1}|x_t, x_0) \quad (1)$$

where  $q_\sigma(x_T|x_0) = \mathcal{N}(\sqrt{\alpha_{T-1}}, (1 - \alpha_T)\mathbf{I})$ . The corresponding reverse process is

$$x_{t-1} = \sqrt{\alpha_{t-1}/\alpha_t} (x_t - \sqrt{1 - \alpha_t} \epsilon_\theta(x_t, t)) + \sqrt{1 - \alpha_{t-1} - \sigma_t^2} \cdot \epsilon_\theta(x_t, t) + \sigma_t \epsilon_t \quad (2)$$

where  $\epsilon_t \sim \mathcal{N}(\mathbf{0}, \mathbf{I})$  is standard Gaussian noise,  $\alpha_t$  is the parameter based on the forward process,  $\sigma_t = \eta \sqrt{(1 - \alpha_{t-1})/(1 - \alpha_t)} \sqrt{1 - \alpha_t/\alpha_{t-1}}$ , and  $\epsilon_\theta(x_t, t)$  is a neural network to predict the noise in  $x_t$ . In this paper, we use a U-Net backbone which is introduced in the supplementary material. When  $\eta = 1$  for all  $t$ , the process of Equation 2 becomes DDPM (Ho et al., 2020). As  $\eta = 0$ , it becomes DDIM and guarantees nearly perfect inversion (Song et al., 2020a).

#### 3.2 Contrastive Language-Image Pre-Training

Contrastive Language-Image Pre-Training (CLIP) (Radford et al., 2021) encapsulates generic and semantic information of image-text pairs. CLIP simultaneously learns an image encoder  $E_I$  and a text encoder  $E_T$  to indicate the similarity between images and texts. StyleGAN-NADA (Gal et al., 2022) produces images guided by a text prompt based on CLIP. Asymp (Kwon et al., 2022) also uses the CLIP to fine tune the pre-trained diffusion model. Inspired by previous works, we adopt CLIP as guidance for the attribute modification:

$$\mathcal{L}_{\text{direction}}(i_{\text{out}}, t_{\text{target}}; i_{\text{edit}}, t_{\text{source}}) := 1 - \frac{\Delta I \cdot \Delta T}{\|\Delta I\| \|\Delta T\|} \quad (3)$$

where  $\Delta I = E_I(i_{\text{out}}) - E_I(i_{\text{edit}})$  and  $\Delta T = E_T(t_{\text{target}}) - E_T(t_{\text{source}})$ , for the generated image  $i_{\text{out}}$ , the editing image  $i_{\text{edit}}$ , the target prompt  $t_{\text{target}}$ , and the source prompt  $t_{\text{source}}$ .

## 4 Method

We present the Zero-shot Inversion Process (ZIP) as a method for attribute editing. The core framework of ZIP is outlined in Section 4.1, where each constituent element of the framework is delineated. Subsequently, the principle of ZIP is elaborated in Section 4.2. Finally, the optimization process and the associated loss function of ZIP are discussed in Section 4.3.

### 4.1 Overview

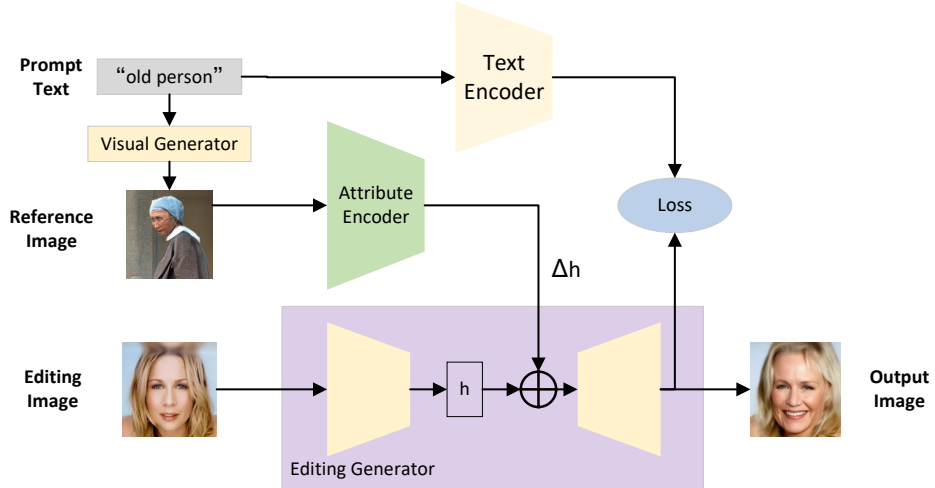


Figure 2: **The framework of ZIP.** A reference image, generated by the Visual Generator, is encoded into edited features denoted as  $\Delta h$ . These edited features are then integrated into the existing features  $h$  of the editing image. The textual prompt contributes semantic information for the manipulation process. To streamline computation, the parameters of both the Attribute Encoder and Editing Generator are shared. During training, updates are exclusively applied to the Attribute Encoder, while the remaining components remain frozen.

We frame the evolution of *any* attribute as a dual-stage process. In the initial stage, a comprehensive diffusion model (referred to as the Editing Generator in ZIP) is trained to capture the foundational features present in images. Leveraging this extensive diffusion model, a lifelike and high-resolution image is synthesized. In the subsequent stage, the Attribute Encoder is trained with the objective of sieving out inconsequential features and seamlessly incorporating the features specific to the designated attribute into the editing images. This two-fold approach proves advantageous for attribute editing, as it ensures the focused extraction and exclusive insertion of attributes.

**Framework:** As depicted in Figure 2, our framework comprises four main components: the Text Encoder, Visual Generator, Attribute Encoder, and Editing Generator. To elaborate, the process unfolds as follows.

Firstly, a textual prompt denoted as  $t$  is constructed based on the specific attribute  $t_{\text{attr}}$ , an example being the prompt "an old person" associated with the "old" attribute.

Subsequently, the Visual Generator generates a reference image  $i_{\text{ref}}$  conditioned on the input  $t$ .

In the third step, attribute features  $\Delta h$  are extracted from  $i_{\text{ref}}$  using the Attribute Encoder. Following this extraction,  $\Delta h$  is integrated into the latent space of the Editing Generator.

The resultant latent representation  $h + \Delta h$  serves as the foundation for generating the target image through the Editing Generator.

**Text Encoder:** To extract textual features, the text prompt  $t$  derived from the attribute  $t_{\text{attr}}$  is encoded into a vector. This vector is subsequently utilized to calculate the CLIP loss in tandem with

the target image. As exemplified by the work of Brown et al. (2020), the evolution of substantial language models has significantly drawn attention to the text prompt, especially in the realm of multimodal applications, e.g., GPT-4 (OpenAI, 2023) and PaLM2 (Google, 2023). These language models have been extensively trained on a vast array of linguistic data and have proven to be adept in few-shot learning scenarios. In this study, the CLIP model (Radford et al., 2021) is employed as the Text Encoder.

In our work, the text prompt  $t$  contains two components:  $t_{\text{source}}$  and  $t_{\text{target}}$ . These components are generated through the following procedure. Let  $E_T$  denote the text encoder equipped with vocabulary  $V$ . The attribute  $t_{\text{attr}}$  constitutes a sequence of phrases denoted as  $t_{\text{attr}} = (s_1, \dots, s_k)$ , where each  $s_i \in V$ . To illustrate with an example, when the attribute  $t_{\text{attr}}$  is “glasses,” the value of  $k$  is 1. Drawing parallels with prompts in natural language processing (NLP) (Schick and Schütze, 2020), we establish the notion of a pattern as a function  $P$ , which takes the attribute  $t_{\text{attr}}$  as input and generates two phrases or sentences,  $t_{\text{source}}$  and  $t_{\text{target}}$ , in the vocabulary  $V$ . This dynamic yields the text prompt  $t = (t_{\text{source}}, t_{\text{target}})$ .

For instance, when the attribute  $t_{\text{attr}}$  pertains to a person, a conceivable pattern could be  $P(t_{\text{attr}}) = (“\text{a person}”, “\text{a person with } t_{\text{attr}}”)$ . Consequently, if the input attribute is  $t_{\text{attr}} = \text{“glasses,”}$  the derived text prompt would be  $P(t_{\text{attr}}) = (“\text{a person}”, “\text{a person with glasses}”)$ , from which  $t_{\text{source}} = \text{“a person”}$  and  $t_{\text{target}} = \text{“a person with glasses.”}$  Collectively, they constitute the comprehensive text prompt  $t$ . After that, the Text Encoder processes this prompt to encode  $t_{\text{source}}$  as  $E_T(t_{\text{source}}) \in \mathbb{R}^d$  and  $t_{\text{target}}$  as  $E_T(t_{\text{target}}) \in \mathbb{R}^d$ .

**Visual Generator:** To acquire the visual attributes corresponding to the specified attribute, we employ a text-image model known as the Visual Generator. Notably, large scale generative models have demonstrated pronounced robustness and adaptability in conditional generation tasks (Saharia et al., 2022; Rombach et al., 2022). While these models may not possess the capacity to pinpoint or precisely modify attributes, they are proficient in generating attribute-associated features within the visual domain. In this study, we adopt UniDiffuser (Bao et al., 2023) as the designated Visual Generator. UniDiffuser uniquely combines text and image generation within a single model, leveraging the concurrent utilization of marginal, conditional, and joint distributions derived from multimodal data.

To acquire the reference image, denoted as  $i_{\text{ref}} = G_V(t_{\text{target}})$ , images are extracted from the conditional distribution  $p(x_0|t_{\text{target}})$  through the following process:

$$p_{\theta}(x_0|t_{\text{target}}) = \int p_{\theta}(x_{0:T}|t_{\text{target}}) dx_{1:T}, \quad p_{\theta}(x_{0:T}|t_{\text{target}}) = p(x_T) \prod_{t=1}^T p_{\theta}(x_{t-1}|x_t, t_{\text{target}}) \quad (4)$$

where  $x_T \sim \mathcal{N}(0, \mathbf{I})$ ,  $p_{\theta}(x_{t-1}|x_t, t_{\text{target}}) = \mathcal{N}(x_{t-1}|\mu_t(x_t, t_{\text{target}}), \sigma_t^2 \mathbf{I})$ , and the mean  $\mu_t = \frac{1}{\sqrt{\alpha_t}}(x_t - \frac{\beta_t}{\sqrt{1-\alpha_t}}\mathbb{E}[\epsilon^x|x_t, t_{\text{target}}])$  is predicted by a noise predictor  $\epsilon_{\theta}$  (Bao et al., 2023). Upon completion of the denoising procedure, we obtain the reference image  $i_{\text{ref}}$ , concluding the process.

**Attribute Encoder:** The Attribute Encoder  $E_A$  functions as a downsampling network, encompassing attention blocks and residual blocks. This type of downsampling network has found wide application in both detection (Ronneberger et al., 2015) and generation (Ho et al., 2020). Through down-sampling, the original image undergoes encoding into a latent space, thereby resulting in a transformed representation. Upon input of the reference image, the Attribute Encoder yields the latent embedding of visual features, i.e.,  $E_A(i_{\text{ref}}) \in \mathbb{R}^D$ . This embedding, represented by  $E_A(i_{\text{ref}})$ , efficiently facilitates attribute manipulation.

**Edit Generator:** The role of the Edit Generator revolves around the generation of the target image. The efficacy of diffusion models has been extensively showcased in prior research (Ho et al., 2020; Choi et al., 2021). In this study, the DDIM model (Song et al., 2020a) is harnessed to generate images, as defined by Equation 2.

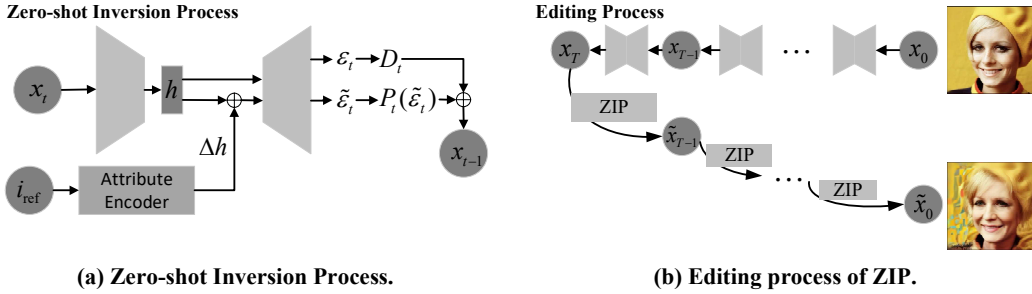


Figure 3: **Zero-shot Inversion Process.** (a) The one step from  $x_t$  to  $x_{t-1}$  in Zero-shot Inversion Process. (b) The inversion process and the forward editing process for a real image.

## 4.2 Zero-shot Inversion Process

Given an image  $i_{\text{edit}} \in \mathbb{R}^{m \times n}$  and an attribute  $t_{\text{attr}}$ , our primary objective is to modify the input image  $i_{\text{edit}}$  in accordance with the attribute  $t_{\text{attr}}$ . This endeavor culminates in the production of an edited image, denoted as  $i_{\text{out}}$ . For instance, envision an image of a person; the user’s intention could involve altering the individual’s age, expression, or attire, while still retaining the human semblance portrayed in the original image.

Figure 3 offers a comprehensive overview of the complete Zero-shot Inversion Process (ZIP), revealing its dual branches: the image-guided branch and the text-guided branch.

Within the image-guided branch, the visual attributes extracted from the reference image  $i_{\text{ref}}$  are integrated into the editing image  $i_{\text{edit}}$  to amplify latent visual attributes that were hitherto unseen. For the generation of the reference image  $i_{\text{ref}}$  under the influence of the prompt condition  $t_{\text{target}}$ , we employ UniDiffuser (Bao et al., 2023). Subsequently, through the utilization of the Attribute Encoder, we extract the corresponding features  $\Delta h = E_A(i_{\text{ref}})$ .

To facilitate latent manipulation on the images  $x_0$  generated from  $x_T$ , a straightforward approach could involve directly modifying the Attribute Encoder to minimize the loss outlined in Equation 3. However, adopting this approach might engender distorted images or erroneous manipulations, as observed in prior works (Choi et al., 2021; Mokady et al., 2022).

An alternative approach entails the modification of the noise  $\epsilon_t^\theta$  anticipated by the network during each sampling iteration. In brief, we can express the abridged version of Equation 2 as follows:

$$x_{t-1} = \sqrt{\alpha_{t-1}} \underbrace{\frac{1}{\sqrt{\alpha_t}} (x_t - \sqrt{1 - \alpha_t} \epsilon_\theta(x_t, t))}_{\text{predicted } x_0, P_t(\epsilon_\theta(x_t, t))} + \underbrace{\sqrt{1 - \alpha_{t-1} - \sigma_t^2} \cdot \epsilon_\theta(x_t, t) + \sigma_t \epsilon_t}_{\text{direction to } x_t, D_t(\epsilon_\theta(x_t, t))} \quad (5)$$

Nonetheless, a direct alteration of the noise  $\epsilon_\theta$  in both  $P_t$  and  $D_t$  leads to mutual nullification, yielding an unchanged  $p_\theta(x_{0:T})$ . This phenomenon mirrors a form of destructive interference, as elucidated in Kwon et al. (2022, Theorem 1).

Hence, in order to circumvent the interference delineated in Equation 2, we resort to the utilization of an asymmetrical controllable reverse process within ZIP:

$$x_{t-1} = \sqrt{\alpha_{t-1}} P_t(\tilde{\epsilon}_\theta(x_t, t)) + D_t(\epsilon_\theta(x_t, t)) + \sigma_t \epsilon_t. \quad (6)$$

Here,  $\tilde{\epsilon}_\theta(x_t, t)$  entails the adjustment of  $\epsilon_\theta(x_t, t)$  grounded on the visual features  $\Delta h$ . This is achieved by introducing  $\Delta h$  into the original feature maps  $h_t$  derived from  $x_t$ .

We depict the attribute editing process for the attribute “glasses” facilitated by ZIP in Figure 4. The accompanying noise maps are showcased. As the temporal step  $t$  progresses, the cumulative noise across 25 steps is visualized within the noise image. Each noise image is derived from a linear extraction throughout the entire generation process. Concurrently, the respective generated images are displayed. Up until  $t = 600$ , no  $\Delta h$  is incorporated into the generation, thereby retaining the original image’s style. After reaching the  $t = 300$  mark, an additional point to note is that, in order to enhance the quality of the generation process,  $\Delta h$  is still not introduced.

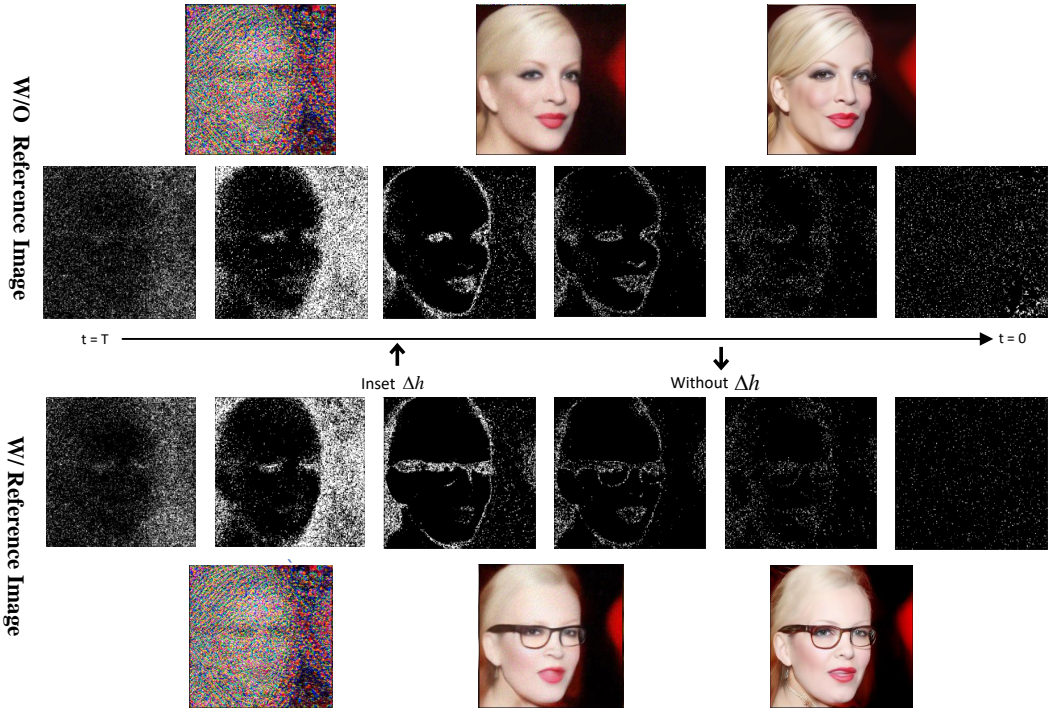


Figure 4: The visualization of noises in ZIP at different time steps  $t$ . The image is edited for the attribute of “glasses.” The top half is the editing process without the reference image while the bottom has the reference image. Pixels are more *concentrated* on the features of the attribute, which implies that the reference image effectively works on generating visual items of the target attribute.

Figure 4 effectively demonstrates that pixels are more *concentrated* on attribute features. This implies the reference image’s efficacy in generating visual components associated with the target attribute. Moreover, in our ZIP process, attribute generation becomes feasible following the insertion of  $\Delta h$ .

### 4.3 Optimization of ZIP

Within the text-guided branch of ZIP, the text prompt  $t$  is harnessed to facilitate the optimization of the ZIP generation process, relying on the CLIP model. Given the absence of ground truth labels in editing tasks, training the model follows a distinct approach compared to conventional vision tasks. As a result, we employ the CLIP loss to fine-tune the network. Aligning with the methodology presented in Avrahami et al. (2022), we employ the directional CLIP loss outlined in Equation 3 as our loss function:

$$\mathcal{L} = \lambda_{\text{clip}} \mathcal{L}_{\text{direction}}(\tilde{P}_t, t_{\text{target}}; P_t, t_{\text{source}}) + \lambda_{\text{recon}} |x_{\text{out}}^t - x_{\text{edit}}^t|. \quad (7)$$

The modified  $\tilde{P}_t$  and the original  $P_t$  correspond respectively to the formulations presented in Equation 6 and Equation 5. Here,  $t_{\text{source}}$  and  $t_{\text{target}}$  reference the text prompts outlined in Section 4.1. The latter expression pertains to the reconstruction loss, which takes the form of the  $L_1$  Loss between the generated image and the original image. This reconstruction loss effectively preserves the original features, thereby averting drastic alterations. To balance the aforementioned losses, the hyperparameters  $\lambda_{\text{clip}}$  and  $\lambda_{\text{recon}}$  are introduced.

During the training phase, the reference image  $i_{\text{ref}}$  and the editing image  $i_{\text{edit}}$  are subject to encoding by the Attribute Encoder and Editing Generator, in accordance with the architecture depicted in Figure 2. Consequently, these encoded representations manifest as  $\Delta h$  and  $h$  in the latent space, respectively.

The resulting output image  $i_{\text{out}}$ , generated by a *frozen* diffusion model (Editing Generator) with input  $\Delta h + h$ , is harnessed for computing the CLIP loss, thereby facilitating the training of the Attribute



Figure 5: **Editing results of ZIP on various datasets.** We conduct experiments on CelebA-HQ, LSUN-church and LSUN-bedroom.

Encoder. In this process, updates are exclusively applied to the parameters of the Attribute Encoder, while the other components, including the Editing Generator, remain *frozen*.

## 5 Experiments

Within this section, we present empirical evidence to substantiate the effectiveness of our Zero-shot Inversion Process (ZIP) in conducting semantic latent editing across diverse attributes and datasets. Section 5.1 delves into the outcomes achieved across various datasets. Additionally, the subsequent section, Section 5.2, features comparative experiments that underscore ZIP’s superior capabilities in semantic editing. This is observed across both in-domain and out-of-domain attributes.

**Baselines.** To facilitate comparison, we implement the ILVR (Choi et al., 2021) and Asyrp (Kwon et al., 2022), as benchmarks against ZIP. ILVR operates as an image-guided approach to semantic synthesis. In the forthcoming experiments, ILVR’s parameters include a low-pass filter scale of  $N = 64$  and a time step of  $t = 100$ . Asyrp, on the other hand, ascertains that diffusion models inherently possess a semantic latent space, rendering it a state-of-the-art text-guided approach. For our Asyrp implementation, we adhere to the default parameters stipulated in the official codebase.

**Implement Details.** All methods, including ZIP, are subjected to training on the CelebA-HQ (Karras et al., 2018), LSUN-church, and LSUN-bedroom datasets (Yu et al., 2015). In the case of ZIP, the Edit Generator draws upon DDPM++ (Song et al., 2020b), and the employed model is sourced from the official pre-trained checkpoint, thus bypassing any training specific to our experiments. Our Visual Generator is realized through Unidiffuser (Bao et al., 2023), while the Text Encoder is represented by the CLIP model (Radford et al., 2021), both using the official checkpoints. Of note, only the last five layers of the Attribute Encoder are subject to training within the ZIP framework. Further details can be explored in the supplementary materials provided.

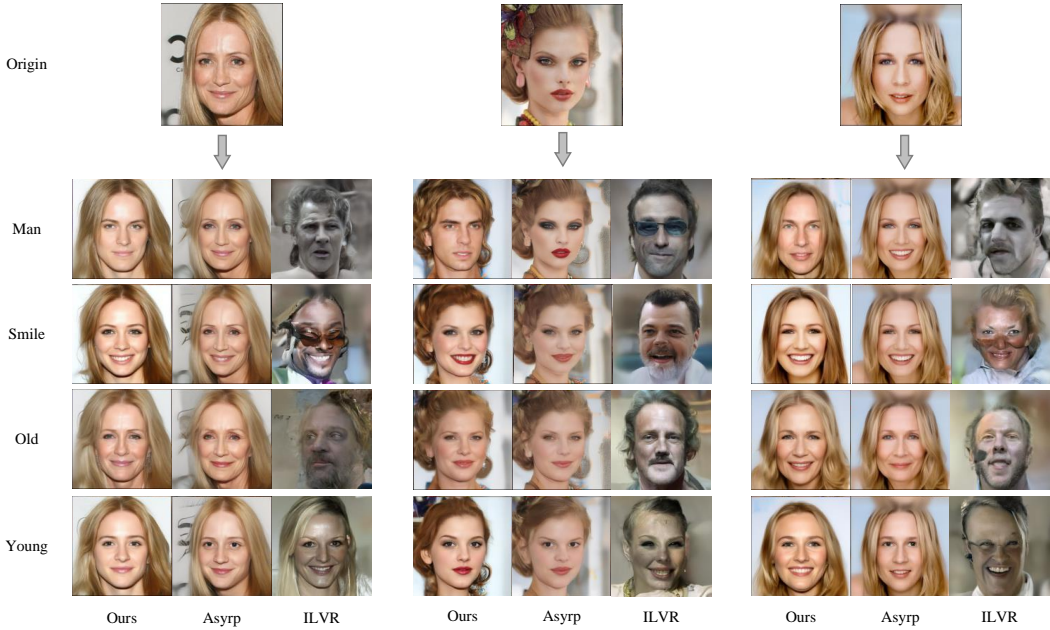


Figure 6: **Editing results for in-domain attributes.** The same attributes are modified by ZIP, Asypr and ILVR.

Table 1: In-domain Attributes Modification

Method	Man			Old			Smiling			Young		
	ISC	FID	CLIP	ISC	FID	CLIP	ISC	FID	CLIP	ISC	FID	CLIP
ILVR (Choi et al., 2021)	2.623	150.2	22.24	2.361	145.1	<b>23.26</b>	2.557	223.7	25.59	2.582	147.9	22.70
Asypr (Kwon et al., 2022)	1.808	77.65	19.15	1.833	77.82	22.73	1.760	73.93	26.31	1.705	80.03	<b>26.11</b>
Ours	1.592	87.31	<b>22.38</b>	1.778	85.96	22.79	1.573	85.36	<b>27.01</b>	1.624	85.28	25.07

**Evaluation.** To assess the proficiency of image generation and editing, prior research has introduced numerous evaluation metrics. In this study, we opt to employ the Inception Score (ISC) (Salimans et al., 2016) and the Fréchet Inception Distance (FID) (Szegedy et al., 2016) as indicators of the image generation quality. Furthermore, the CLIP Score (Radford et al., 2021) is leveraged to gauge the alignment between edited images and their intended semantic targets.

## 5.1 Visualization Results

Figure 5 illustrates the visual outcomes attained through our methodology across diverse datasets. ZIP demonstrates its capacity to synthesize attributes present within the training datasets, such as age and gender in CelebA-HQ. Additionally, it can manipulate attributes based on the semantics provided by the text prompt, exemplified by “gothic” in LSUN-church. This versatility in semantic synthesis showcases ZIP’s ability to accomplish varied tasks solely through training with distinct text prompts.

## 5.2 In-domain an Out-of-domain Attribute

In our evaluation, ZIP is assessed from two perspectives. Firstly, we scrutinize its performance in manipulating attributes that are inherently present within the datasets. For instance, in CelebA-HQ, numerous images feature individuals with smiling expressions, and the attribute of “smiling” is explicitly labeled in the datasets. For the purposes of this evaluation, we refer to these attributes as “In-domain Attributes.” Conversely, we examine attributes that are not explicitly represented in the datasets, such as “Add glasses.” These are referred to as “Out-of-domain Attributes.”

Figure 6 presents the outcomes of our method concerning in-domain attributes, juxtaposed with results from ILVR and Asypr. Our approach successfully alters specific attributes while keeping

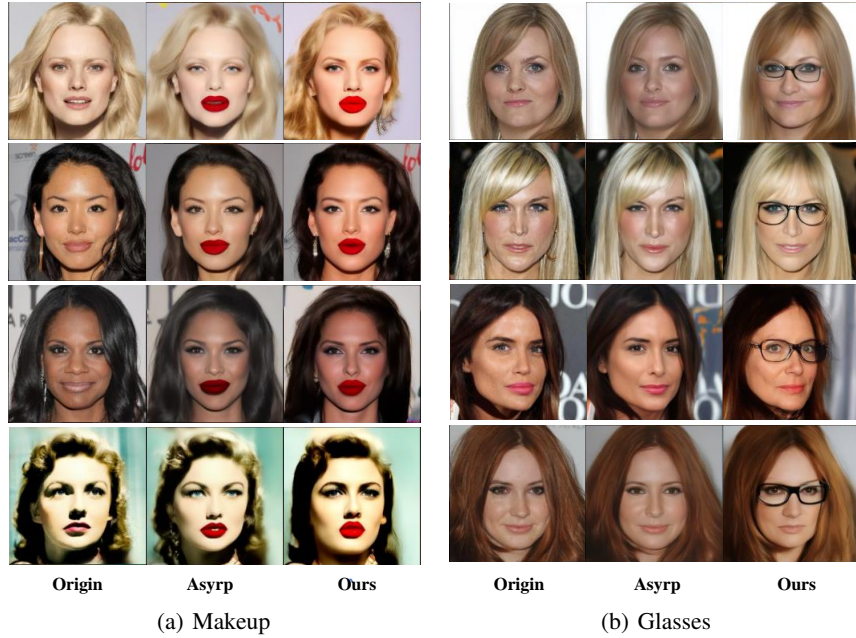


Figure 7: **Editing results for out-of-domain attributes.**

Table 2: Out-of-domain Attributes Modification

Method	Glasses			Makeup		
	ISC	FID	CLIP	ISC	FID	CLIP
ILVR (Choi et al., 2021)	1.940	144.4	24.10	3.060	165.6	24.52
Asyrrp (Kwon et al., 2022)	1.755	77.49	23.86	1.390	147.5	29.55
Ours	1.467	108.0	<b>25.12</b>	1.418	154.6	<b>30.07</b>

other attributes constant. This includes modifying expressions of individuals. In the context of text-guided approaches like Asyrrp, attributes that don’t necessitate alterations in visual features are handled adeptly. For example, attributes like “smiling,” which entail facial feature deformations, can be effectively edited by Asyrrp. However, altering attributes like gender demands replacing female features with male features, a feat that cannot be accomplished solely through text-guided methods. Meanwhile, for image-guided approaches such as ILVR, the relationship between the target attribute and the reference image can be less defined. Consequently, ILVR is prone to producing distorted or inaccurately manipulated images, as depicted in Figure 6. ZIP’s strength lies in its capacity to synergize textual prompts with reference images to yield high-quality edits across a diverse array of attributes. The outcomes displayed in Table 1 corroborate this, demonstrating that ZIP achieves superior editing outcomes for attributes, without compromising on quality, when compared to alternative methods.

Figure 7 portrays the outcomes pertaining to out-of-domain attributes, such as the addition of glasses and alteration of makeup. ZIP consistently achieves the highest CLIP scores across all attributes, a fact corroborated by the data presented in Table 2. As observed with in-domain attributes, Asyrrp’s performance is impeded by its inability to access additional visual features. Conversely, ZIP demonstrates its competence in generating novel attributes by leveraging the capabilities of the Visual Generator and Text Encoder. This facilitates the generalization of both visual and semantic information, rendering ZIP highly proficient in addressing out-of-domain attributes.

## 6 Conclusion

This paper introduces ZIP, a novel approach for the manipulation of real-world images using natural language. ZIP achieves this by infusing a blend of generated visual reference and textual guidance

into the semantic latent space of a *frozen* diffusion model. By bridging the gap between visual patterns and textual semantics, ZIP is capable of effectively altering attributes, irrespective of whether they are in-domain or out-of-domain. In the future, our research will delve into enhancing the accuracy of attribute acquisition from reference images. This involves refining methods for specifying attributes with similar visual features, thus further improving the manipulation process.

**Limitation.** Indeed, while ZIP excels in producing realistic edits for real images, it's important to acknowledge that it faces a limitation in the absence of a target mask, similar to the capability demonstrated by Imagen Editor (Wang et al., 2022). Imagen Editor's ability to use an editing mask as input allows it to achieve intensive and precise editing of the target attributes. On the other hand, ZIP's operation without a clearly defined mask might lead to inadvertent alignment of visual features and text prompts, potentially resulting in incorrect or unintended modifications. This points to an avenue for improvement in the future, as addressing this limitation could further enhance ZIP's editing accuracy.

## References

Avrahami, O., Lischinski, D., and Fried, O. (2022). Blended diffusion for text-driven editing of natural images. In *Proceedings of the IEEE/CVF Conference on Computer Vision and Pattern Recognition*, pages 18208–18218.

Bao, F., Nie, S., Xue, K., Li, C., Pu, S., Wang, Y., Yue, G., Cao, Y., Su, H., and Zhu, J. (2023). One transformer fits all distributions in multi-modal diffusion at scale. *arXiv preprint arXiv:2303.06555*.

Brown, T., Mann, B., Ryder, N., Subbiah, M., Kaplan, J. D., Dhariwal, P., Neelakantan, A., Shyam, P., Sastry, G., Askell, A., et al. (2020). Language models are few-shot learners. *Advances in neural information processing systems*, 33:1877–1901.

Choi, J., Kim, S., Jeong, Y., Gwon, Y., and Yoon, S. (2021). Ilvr: Conditioning method for denoising diffusion probabilistic models. *arXiv preprint arXiv:2108.02938*.

Dasas, G. and Dimakis, A. G. (2022). Multiresolution textual inversion. *arXiv preprint arXiv:2211.17115*.

Elarabawy, A., Kamath, H., and Denton, S. (2022). Direct inversion: Optimization-free text-driven real image editing with diffusion models. *arXiv preprint arXiv:2211.07825*.

Gal, R., Patashnik, O., Maron, H., Bermano, A. H., Chechik, G., and Cohen-Or, D. (2022). Stylegan-nada: Clip-guided domain adaptation of image generators. *ACM Transactions on Graphics (TOG)*, 41(4):1–13.

Google (2023). Palm 2 technical report.

Hertz, A., Mokady, R., Tenenbaum, J., Aberman, K., Pritch, Y., and Cohen-Or, D. (2022). Prompt-to-prompt image editing with cross attention control. *arXiv preprint arXiv:2208.01626*.

Heusel, M., Ramsauer, H., Unterthiner, T., Nessler, B., and Hochreiter, S. (2017a). Gans trained by a two time-scale update rule converge to a local nash equilibrium. *Advances in neural information processing systems*, 30.

Heusel, M., Ramsauer, H., Unterthiner, T., Nessler, B., and Hochreiter, S. (2017b). Gans trained by a two time-scale update rule converge to a local nash equilibrium. *Advances in neural information processing systems*, 30.

Ho, J., Jain, A., and Abbeel, P. (2020). Denoising diffusion probabilistic models. *Advances in Neural Information Processing Systems*, 33:6840–6851.

Jia, X., Zhao, Y., Chan, K. C., Li, Y., Zhang, H., Gong, B., Hou, T., Wang, H., and Su, Y.-C. (2023). Taming encoder for zero fine-tuning image customization with text-to-image diffusion models. *arXiv preprint arXiv:2304.02642*.

Karras, T., Aila, T., Laine, S., and Lehtinen, J. (2018). Progressive growing of gans for improved quality, stability, and variation. In *International Conference on Learning Representations*.

Karras, T., Laine, S., Aittala, M., Hellsten, J., Lehtinen, J., and Aila, T. (2020). Analyzing and improving the image quality of stylegan. In *Proceedings of the IEEE/CVF conference on computer vision and pattern recognition*, pages 8110–8119.

Kim, G., Kwon, T., and Ye, J. C. (2022). Diffusionclip: Text-guided diffusion models for robust image manipulation. In *Proceedings of the IEEE/CVF Conference on Computer Vision and Pattern Recognition*, pages 2426–2435.

Kwon, M., Jeong, J., and Uh, Y. (2022). Diffusion models already have a semantic latent space. *arXiv preprint arXiv:2210.10960*.

Lugmayr, A., Danelljan, M., Romero, A., Yu, F., Timofte, R., and Van Gool, L. (2022). Repaint: Inpainting using denoising diffusion probabilistic models. In *Proceedings of the IEEE/CVF Conference on Computer Vision and Pattern Recognition*, pages 11461–11471.

Meng, C., He, Y., Song, Y., Song, J., Wu, J., Zhu, J.-Y., and Ermon, S. (2021). Sdedit: Guided image synthesis and editing with stochastic differential equations. In *International Conference on Learning Representations*.

Mokady, R., Hertz, A., Aberman, K., Pritch, Y., and Cohen-Or, D. (2022). Null-text inversion for editing real images using guided diffusion models. *arXiv preprint arXiv:2211.09794*.

Nitzan, Y., Aberman, K., He, Q., Liba, O., Yarom, M., Gandsman, Y., Mossner, I., Pritch, Y., and Cohen-Or, D. (2022). Mystyle: A personalized generative prior. *ACM Transactions on Graphics (TOG)*, 41(6):1–10.

OpenAI (2023). Gpt-4 technical report.

Radford, A., Kim, J. W., Hallacy, C., Ramesh, A., Goh, G., Agarwal, S., Sastry, G., Askell, A., Mishkin, P., Clark, J., et al. (2021). Learning transferable visual models from natural language supervision. In *International conference on machine learning*, pages 8748–8763. PMLR.

Ramesh, A., Pavlov, M., Goh, G., Gray, S., Voss, C., Radford, A., Chen, M., and Sutskever, I. (2021). Zero-shot text-to-image generation. In *International Conference on Machine Learning*, pages 8821–8831. PMLR.

Rombach, R., Blattmann, A., Lorenz, D., Esser, P., and Ommer, B. (2022). High-resolution image synthesis with latent diffusion models. In *Proceedings of the IEEE/CVF Conference on Computer Vision and Pattern Recognition*, pages 10684–10695.

Ronneberger, O., Fischer, P., and Brox, T. (2015). U-net: Convolutional networks for biomedical image segmentation. In *Medical Image Computing and Computer-Assisted Intervention–MICCAI 2015: 18th International Conference, Munich, Germany, October 5–9, 2015, Proceedings, Part III* 18, pages 234–241. Springer.

Saharia, C., Chan, W., Saxena, S., Li, L., Whang, J., Denton, E. L., Ghasemipour, K., Gontijo Lopes, R., Karagol Ayan, B., Salimans, T., et al. (2022). Photorealistic text-to-image diffusion models with deep language understanding. *Advances in Neural Information Processing Systems*, 35:36479–36494.

Salimans, T., Goodfellow, I., Zaremba, W., Cheung, V., Radford, A., and Chen, X. (2016). Improved techniques for training gans. *Advances in neural information processing systems*, 29.

Schick, T. and Schütze, H. (2020). Exploiting cloze questions for few shot text classification and natural language inference. *arXiv preprint arXiv:2001.07676*.

Song, J., Meng, C., and Ermon, S. (2020a). Denoising diffusion implicit models. *arXiv preprint arXiv:2010.02502*.

Song, Y., Sohl-Dickstein, J., Kingma, D. P., Kumar, A., Ermon, S., and Poole, B. (2020b). Score-based generative modeling through stochastic differential equations. *arXiv preprint arXiv:2011.13456*.

Szegedy, C., Vanhoucke, V., Ioffe, S., Shlens, J., and Wojna, Z. (2016). Rethinking the inception architecture for computer vision. In *Proceedings of the IEEE conference on computer vision and pattern recognition*, pages 2818–2826.

Wallace, B., Gokul, A., and Naik, N. (2022). Edict: Exact diffusion inversion via coupled transformations. *arXiv preprint arXiv:2211.12446*.

Wang, S., Saharia, C., Montgomery, C., Pont-Tuset, J., Noy, S., Pellegrini, S., Onoe, Y., Laszlo, S., Fleet, D. J., Soricut, R., et al. (2022). Imagen editor and editbench: Advancing and evaluating text-guided image inpainting. *arXiv preprint arXiv:2212.06909*.

Yu, F., Seff, A., Zhang, Y., Song, S., Funkhouser, T., and Xiao, J. (2015). Lsun: Construction of a large-scale image dataset using deep learning with humans in the loop. *arXiv preprint arXiv:1506.03365*.

## Supplementary Material

### Zero-shot Inversion Process for Image Attribute Editing with Diffusion Models

## A Useful Lemmas

**Theorem 1 (Kwon et al. (2022, Theorem 1))** Let  $\epsilon_t^\theta$  be a predicted noise during the original reverse process at  $t$  and  $\tilde{\epsilon}_t^\theta$  be its shifted counterpart. Then,  $\tilde{x}_{t-1} \approx x_{t-1}$  where  $\tilde{x}_{t-1} = \sqrt{\alpha_{t-1}} P_t(\tilde{\epsilon}_t^\theta(x_t)) + D_t(\tilde{\epsilon}_t^\theta(x_t))$ . I.e., the shifted terms of  $\tilde{\epsilon}_t^\theta$  in  $P_t$  and  $D_t$  destruct each other in the reverse process.

## B Experiment Details

### B.1 Parameters

The parameters of our ZIP in different datasets are shown in Table 3. The code is also attached to the supplementary materials.

Table 3: The parameters of ZIP

Parameter	CelebA-HQ	LSUN-church	LSUN-bedroom
Resolution of images	256×256	256×256	256×256
Time step $T$	1000	1000	1000
Batch size of training	9	9	9
Inversion time step	40	40	40
Learning rate of training	0.5	0.5	0.5
The weight of visual features $\Delta h$	0.3	0.1	0.1
The weight of CLIP loss $\lambda_{\text{clip}}$	0.8	2	0.8
The weight of reconstruction loss $\lambda_{\text{recon}}$	3	3	3

### B.2 Evaluation

**Inception Score:** Inception Score (ISC) (Salimans et al., 2016) is used to access how realistic generated images are. The computation of ISC is:

$$ISC = \exp(\mathbb{E}_x KL(p(y|x) || p(y))) \quad (8)$$

where  $KL(p(y|x) || p(y))$  is the KL divergence between the conditional distribution  $p(y|x)$  and the marginal distribution  $p(y)$ . Both the conditional and marginal distribution is calculated from features extracted from the images. The score is calculated on random splits of the images such that both a mean and standard deviation of the score are returned. In this paper, ISC is computed based on the original weights from (Heusel et al., 2017a).

**Fréchet Inception Distance:** Fréchet Inception Distance (FID) (Szegedy et al., 2016) also is used to access the quality of generated images. Different from ISC, which is computed only by the generated images ignoring the real images, FID uses the features from Inception Network to evaluate the similarity of real images and generated images. FID is computed by:

$$FID = |\mu - \mu_\omega| + \text{tr}(\Sigma + \Sigma_\omega - 2(\Sigma \Sigma_\omega)^{\frac{1}{2}}) \quad (9)$$

where  $\mathcal{N}(\mu, \Sigma)$  is the multivariate normal distribution estimated from Inception v3 (Szegedy et al., 2016) features calculated on real life images and  $\mathcal{N}(\mu_\omega, \Sigma_\omega)$  is the multivariate normal distribution estimated from Inception v3 features calculated on generated images. In this paper, FID is computed based on the original weights from (Heusel et al., 2017b).

**CLIP Score:** CLIP Score (Radford et al., 2021) is a reference-free metric that can be used to evaluate the correlation between a generated caption for an image and the actual content of the image. It has been found to be highly correlated with human judgment. The metric is defined as:

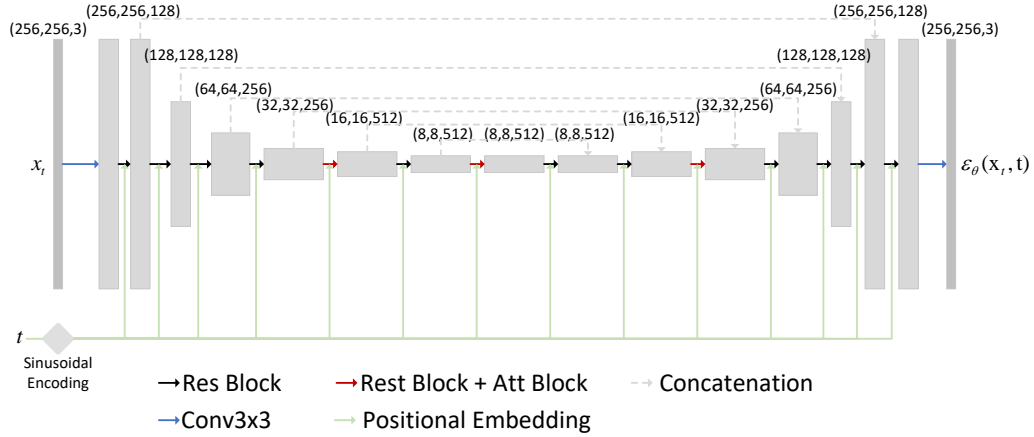


Figure 8: **The Architecture of Editing Generator.** The U-Net architecture of Editing Generator outputs  $256 \times 256$  images. The  $\Delta h$  is inserted into the middle layer.



Figure 9: **The results in LSUN-bedroom.**

$$extCLIPScore(i, c) = \max(100 * \cos(E_i, E_c), 0) \quad (10)$$

which corresponds to the cosine similarity between visual CLIP embedding  $E_i$  for an image  $i$  and textual CLIP embedding  $E_c$  for an caption  $c$ . In the following experiments, the model "clip-vit-base-patch16" from official checkpoints of CLIP model (Radford et al., 2021) is used to evaluate the attribute changes.

In our experiments, we use the code of torch-fidelity<sup>†</sup> to compute ISC and FID. CLIP Score is computed based on TorchMetrics<sup>†</sup>.

## C Network Architecture

### C.1 Attribute Encoder and Editing Generator

We use a U-net backbone as our Editing Generator as shown in Figure 8. The Attribute Encoder shares parameters with the Editing Generator in the down-sampling parts (the first eight layers). In the training process, we only update the parameters of the Attribute Encoder.

<sup>†</sup> <https://github.com/toshas/torch-fidelity>.

<sup>†</sup> [https://torchmetrics.readthedocs.io/en/stable/multimodal/clip\\_score.html](https://torchmetrics.readthedocs.io/en/stable/multimodal/clip_score.html).



Figure 10: The results in LSUN-church.

Table 4: The results of LSUN dataset

Method	gothic				night				department				factory				bedroom-hotel			
	ISC	FID	CLIP	ISC	FID	CLIP	ISC	FID	CLIP	ISC	FID	CLIP	ISC	FID	CLIP	ISC	FID	CLIP		
Asyryp (Kwon et al., 2022)	2.769	93.13	21.98	3.198	111.4	22.05	3.290	118.3	<b>23.49</b>	3.175	109.7	22.15	2.033	102.5	24.64					
Ours	2.958	118.0	<b>24.24</b>	3.486	209.9	<b>23.24</b>	2.631	112.0	23.21	3.346	133.7	<b>22.92</b>	2.599	115.5	<b>26.52</b>					

## C.2 Others

The other parts of our framework are frozen with the official checkpoints. We use Unidiffuser (Bao et al., 2023) and CLIP model (Radford et al., 2021) as the Visual Generator and the Text Encoder with the official checkpoints, respectively.

## D More Results

We supply more results for different datasets, such as LSUN-church in Figure 10 LSUN-bedroom in Figure 9, and CelebA-HQ in in Figure 14. The other attributes for different datasets, such as “Department” and “Factory”, are shown in a bigger size.

In Figure 11 and Figure 12, we show more results in test data for the in-domain attribute “gender” and “smile”. For visual features, ZIP can generate extra features of gender. For the deformation of facial features, ZIP can also change the original features well. Moreover, in Figure 13, the out-of-domain attribute is shown.

Also, as Figure 15 shows, the top half is the editing process for the attribute “makeup” without the reference image while the bottom has the reference image. Though both of them generate the details of the face, the results with the reference image are more *concentrated* on the features of the attribute “makeup”, such as the part of lips.



Figure 11: The results in CelebA-HQ for the attribute “gender”.



Figure 12: The results in CelebA-HQ for the attribute “smile”.



Figure 13: The results in CelebA-HQ for the attribute “makeup”.



Figure 14: The results in CelebA-HQ.

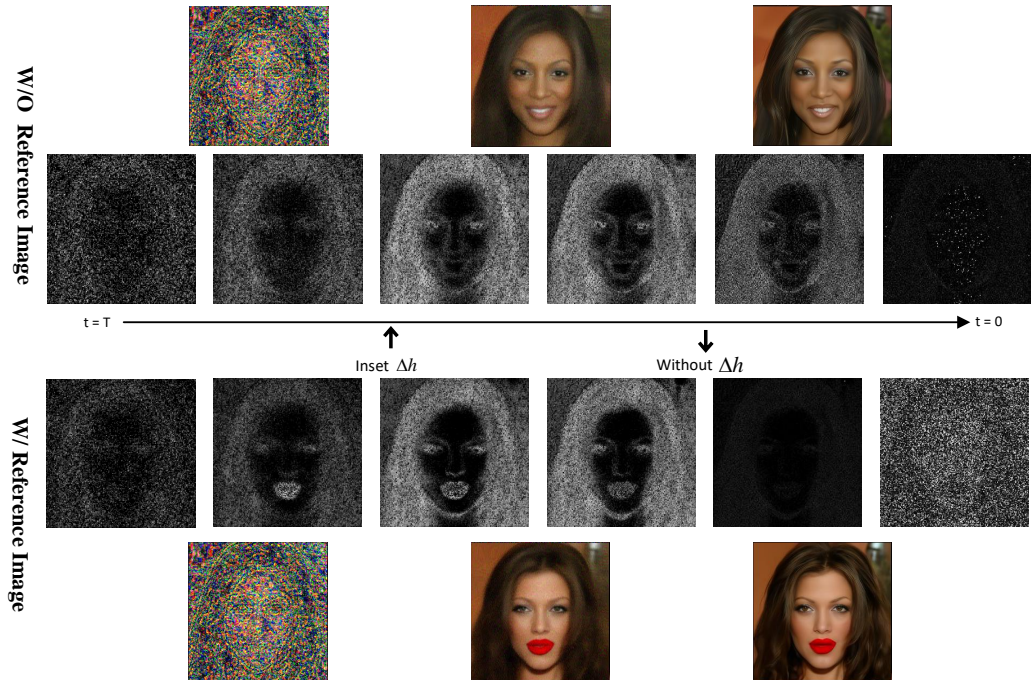


Figure 15: The visualization of noises in ZIP at different time steps  $t$ . The image is edited for the attribute of “makeup.”